

Hessian matrix approach for determining error field sensitivity to coil deviations

Caoxiang Zhu, Stuart R. Hudson, Samuel A. Lazerson & David A. Gates

Princeton Plasma Physics Laboratory

Thanks to: F. Volpe (Columbia Univ.), J. Geiger, K. Hammond, T. S. Pedersen (IPP), Yuntao Song (ASIPP), Yuanxi Wan (USTC)

Motivations

Error field control is crucial for stellarators.

❖ Error field (EF) is vital for magnetically confined fusion devices.

- Plasma is sensitive to small magnetic perturbations, even as small as $\delta B/B \approx 10^{-4}$
- EF is mainly produced by the inevitable coil misalignments, including ([La Haye et al. 1992](#))
 - “as-designed” irregularities
 - “as-built” misplacements
 - others

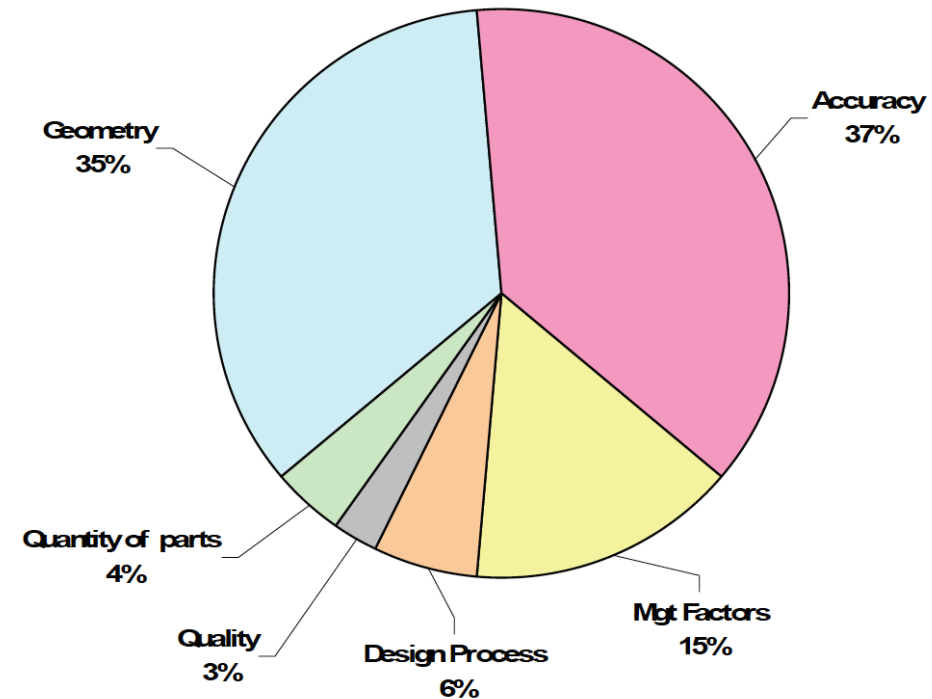
❖ EF control is more critical for stellarators.

- Main (all) magnetic field is provided by external coils
- Coils are more complicated (non-planar, twisted, wiggles)
- Lessons learned from NCSX stellarator:

“The largest driver of the project cost growth were the accuracy requirements required for fabrication and assembly of the Stellarators core.” ---- Strykowsky et al. 2009

❖ Numerical efforts provide insights for avoiding deleterious EFs prior constructions.

Much cheaper, “Hazards forecast”, Improve designs

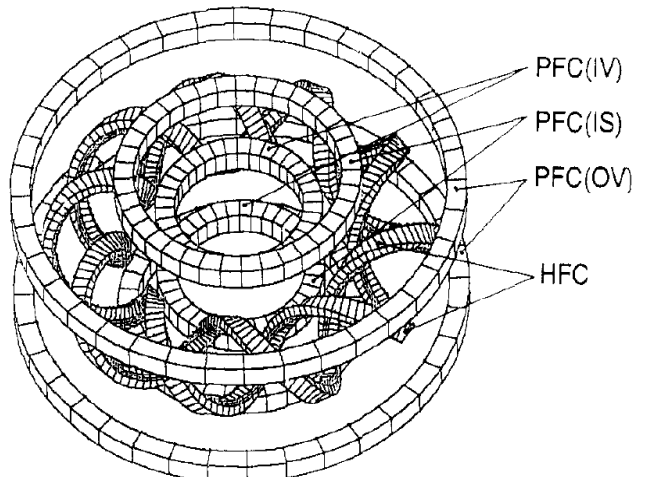


Cost growth by category.

Studies on accuracy requirements of LHD coils.

❖ LHD superconducting coils

3 pairs of PF coils
2 helical windings

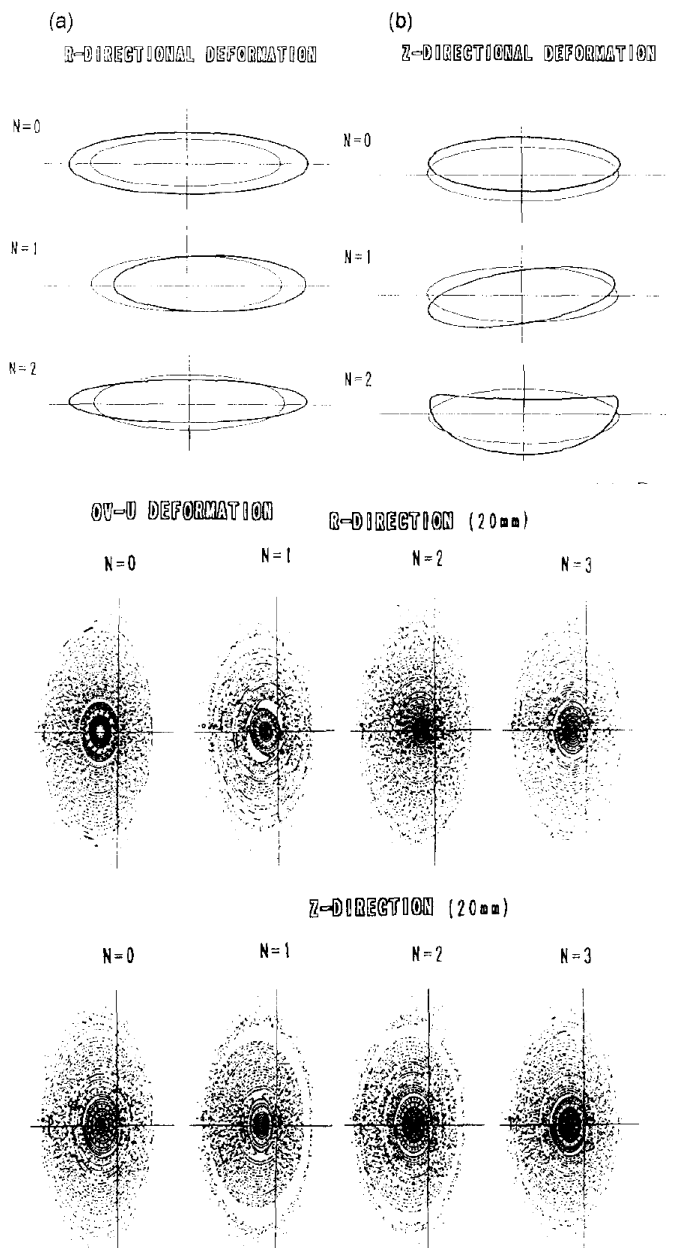


❖ Deformation of the coil system

Global deformation of PF coils

$$\begin{aligned} X &= R_0 \cos \phi, & X &= [R_0 + \Delta_R \cos(N_R \phi + \phi_0)] \cos \phi, \\ Y &= R_0 \sin \phi, & \longrightarrow & Y = [R_0 + \Delta_R \cos(N_R \phi + \phi_0)] \sin \phi, \\ Z &= Z_0, & & Z = \Delta_Z \cos(N_Z \phi + \phi_0). \end{aligned}$$

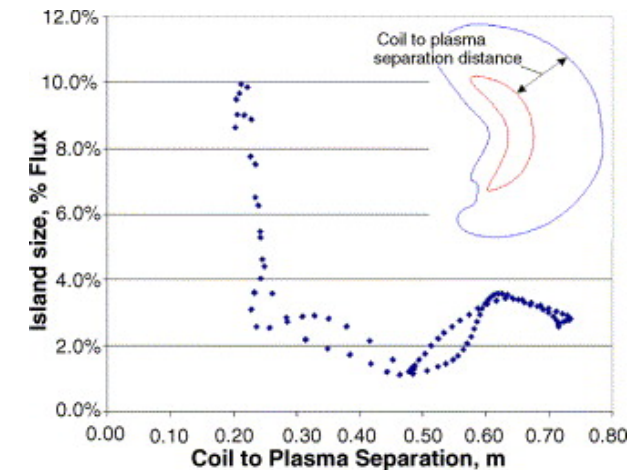
N=1 the most dangerous; N>3 negligible



Error field sensitivity analysis on NCSX and W7-X.

❖ Gauge the severity of winding errors in the final coil assembly of NCSX¹

- A Fourier representation in which the local tolerance varies with coil-plasma spacing;
- A short wavelet type displacement in orthogonal directions to the winding center;
- A broad displacement over a significant length of the coil.



❖ Correct error field during the assembly of W7-X²

- Calculate the distinct Fourier spectra when defined shifts are applied on each module.
- Offset alignments for all the modules to correct the measured EFs produced by manufacturing errors.
- Together with other efforts, i.e. correction coils, high-precision manufacture techniques, etc, the measured deviations are smaller than one part in 100,000 (*Pedersen et al. 2016*)

1.5 mm broad out-of-plane distortions in the coil arise island.

	B_{11}	B_{22}	B_{33}	B_{44}
Shift in X	0.13	0.063	0.03	0.017
Shift in Y	0.17	0.09	0.04	0.017
Shift in Z	0.12	0.043	0.027	0.017
α	2.76	1.43	0.64	0.26
β	1.22	0.45	0.27	0.18
γ	0.39	0.14	0.087	0.063

Fourier components in units $10^{-4}/B_{00}$ generated if distinct shifts (1 cm) and inclination angles (1°) are applied to the modules no. 1 located between $\phi = \pm 36^\circ$

New numerical approaches are being developed.

❖ Shape gradient used for computing local sensitivity and tolerance.

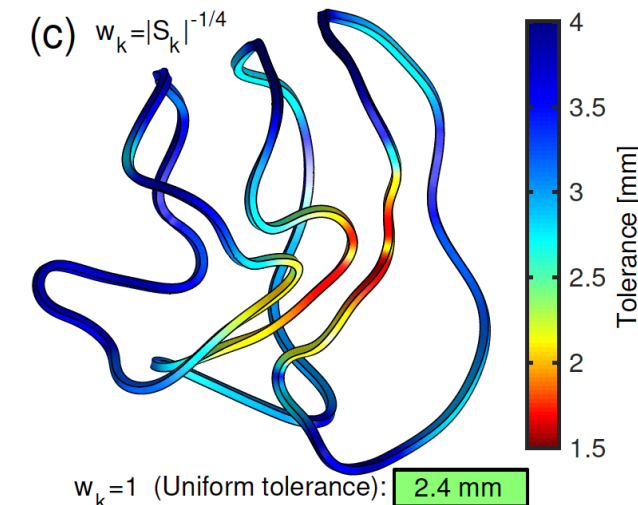
- The tangent components are vanished in shape gradient

$$\int_0^{2\pi} d\vartheta \left| \frac{dr}{d\vartheta} \right| \frac{\partial r}{\partial p_j} \cdot S = \frac{\partial f}{\partial p_j}$$

- Use the shape gradient to compute coil tolerance.

$$T_k(\ell) = \frac{w_k(\ell) \Delta f}{\sum_{k'} \int d\ell' w_{k'}(\ell') |S_{k'}(\ell')|},$$

- Details were shown in P1.031 (*Landreman & Paul, 2018*)



Shape tolerance required to achieve $\Delta t < 0.02$

Our approach: Hessian matrix method using FOCUS*.

* FOCUS = Flexible Optimized Coils Using Space curves

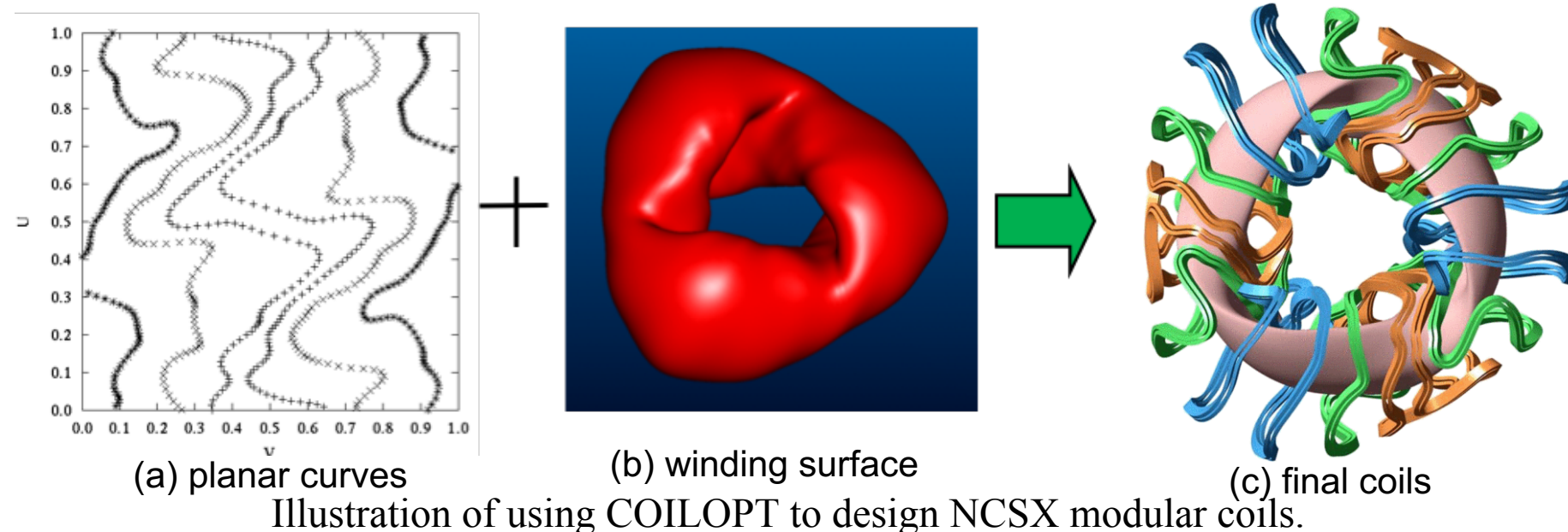
FOCUS introduction

Zhu, et al. Nuclear Fusion 58 (2017) 016008

Zhu, et al. Plasma Physics and Controlled Fusion 60 (2018) 065008

Previous coil design methods require a defined winding surface.

- ❖ For given magnetic field, how can we find appropriate coils? (ill-posed, non-unique problem)
- ❖ Green's function to solve a continuous current potential (NESCOIL, NESVSD, REGCOIL)
- ❖ Nonlinear optimization to simplify engineering complexities (ONSET, COILOPT, COILOPT++)



- ❖ Additional optimizations for the winding surface
 - Uniformly expand the plasma boundary
 - Adjust by experience
 - Interpolation between two constrained surfaces
 - Adjoint method (*Paul et al. P3.031*)

FOCUS adopts 3D representation to describe coils directly.

❖ Get rid of the need of winding surface by describing coils in 3D space.

➢ Simplify coils as single filaments (zero cross-sectional area)

➢ Fourier representation in Cartesian coordinates

$$x(t) = X_{c,0} + \sum_{n=1}^{N_F} [X_{c,n} \cos(nt) + X_{s,n} \sin(nt)]$$

Fourier angle $t \in [0, 2\pi]$, likewise for $y(t), z(t)$.

- ✓ general, differentiable
- ✓ global, smooth

➢ Piecewise linear representation is also being developed

$$\mathbf{P}_1(x_1, y_1, z_1) \ \mathbf{P}_2(x_2, y_2, z_2) \ \dots \ \mathbf{P}_n(x_n, y_n, z_n)$$

➢ Other representations, i.e. cubic spline, remaining for future development.

- ✗ not efficient for straight
- ✗ not unique

- ✓ general, local
- ✓ numerical convenience

- ✗ more DoF
- ✗ only 0-order continuous

❖ All the degrees of freedom are packed into one array.

$$\mathbf{X} = \left[\underbrace{X_{c,0}^1, \dots, X_{c,N}^1}_{N+1}, \underbrace{X_{s,1}^1, \dots, X_{s,N}^1}_N, \overbrace{Y_{c,0}^1, \dots, Z_{s,N}^1, I^1}^{6N+4}, \dots, \dots, X_{c,0}^{N_c}, \dots, I^{N_c} \right]$$

Coils are designed to generate desired magnetic field.

- ❖ External magnetic field within a region enclosed by a toroidal surface can be uniquely determined by

- 1) the normal magnetic field on the torus;
- 2) the net toroidal magnetic flux within the torus.

- ❖ Match the normal field

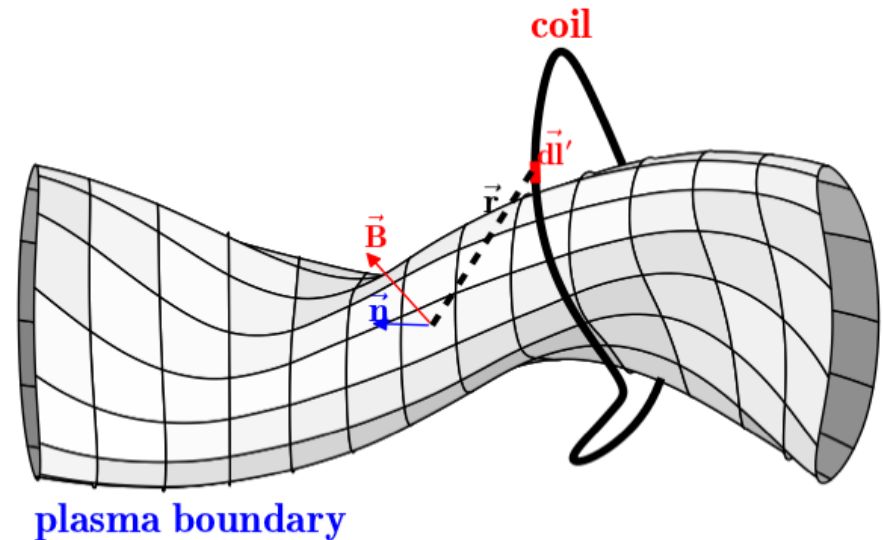
Minimize the residual errors

$$f_B(\mathbf{X}) \equiv \int_S \frac{1}{2} (\mathbf{B}_V \cdot \mathbf{n} - T_{Bn})^2 ds$$

\mathbf{B}_V : vacuum field generated by coils

T_{Bn} : target B_n distribution

$$\mathbf{B}_V(\bar{\mathbf{x}}) = \frac{\mu_0}{4\pi} \sum_{i=1}^{N_C} I_i \int_{C_i} \frac{d\mathbf{l}_i \times \mathbf{r}}{r^3}$$



- ❖ Produce the toroidal flux

$$f_\Psi(\mathbf{X}) \equiv \frac{1}{2\pi} \int_0^{2\pi} \frac{1}{2} \left(\frac{\Psi_\zeta - \Psi_o}{\Psi_o} \right)^2 d\zeta$$

Ψ_ζ : toroidal flux at $\zeta=\text{const.}$ Ψ_0 : target toroidal flux

Coils have to be constructable.

❖ Coil length

With finite number of coils, to reduce B_n residual errors, coils tend to

- Further away from plasma meanwhile increasing the currents (lower ripple)
- More wiggles (better fit plasma)

Constraint / Pernaly function on coil length

$$f_L = \frac{1}{N_C} \sum_{i=1}^{N_C} \frac{e^{L_i}}{e^{L_{i,o}}} \quad \text{OR} \quad f_L = \frac{1}{N_C} \sum_{i=1}^{N_C} \frac{1}{2} \frac{(L_i - L_{i,o})^2}{L_{i,o}^2}$$

❖ Coil to coil separation

Actual coil has finite width. Adjacent coils cannot intersect.

$$f_C = \sum_{i,j} \int_{C_i} \int_{C_j} \frac{dl_i dl_j}{|\mathbf{r}_i - \mathbf{r}_j|^2}$$

differentiable

❖ Coil to surface separation

Sufficient space between coils and the plasma

$$E(\mathcal{C}, \mathcal{S}) \equiv \oint_{\mathcal{S}} \int_{\mathcal{C}} \frac{ds dl}{|\mathbf{x}_c - \mathbf{x}_s|^q} , \quad f_S(\mathbf{X}) = \sum_{i=1}^{N_{coils}} E(\mathcal{C}_i, \mathcal{S})$$

Nonlinear opt. algorithms to minimize the target function.

- ❖ **Target function comprises multiple cost functions.**

- Coil parameters are varied to satisfy multiple objective functions.
- Both **physics requirements** and **engineering constraints** are considered.
- Objective functions can be **arbitrarily** constructed.

$$\min_{\mathbf{X} \in \mathbb{R}^n} \chi^2(\mathbf{X}) = \sum_i w_i \left(\frac{f_i(\mathbf{X}) - f_{i,o}}{f_{i,o}} \right)^2$$

- ❖ **Different optimization algorithms are applied.**

Gradient-based algorithms

- Differential/Gradient Flow
- Nonlinear Conjugate Gradient

Hessian-based algorithms

- Modified Newton Method
- Hybrid Powell Method
- Truncated Newton Method

FOCUS analytically computes the 1st & 2nd derivatives.

- ❖ **Gradient and/or Hessian is needed in most minimization algorithms.**
 - FOCUS employs **differentiable** coil representation and **carefully chosen** objective functions.
 - Rather than finite difference, FOCUS could compute the derivatives analytically (albeit a little complicated).
- ❖ **Example of calculating the 1st and 2nd derivatives of f_B**

A simplified form of f_B :

$$f_B(\mathbf{X}) \equiv \int_S \frac{1}{2} (\mathbf{B} \cdot \mathbf{n})^2 ds$$

For an arbitrary variable, $\forall X_m \in \mathbf{X}$, we have

$$\frac{\partial f_B}{\partial X_m} = \int_S (\mathbf{B} \cdot \mathbf{n}) \left(\frac{\partial \mathbf{B}_V}{\partial X_m} \cdot \mathbf{n} \right) ds$$

$$\frac{\partial^2 f_B}{\partial X_m^2} = \int_S \left(\frac{\partial \mathbf{B}_V}{\partial X_m} \cdot \mathbf{n} \right)^2 + \left(\frac{\partial^2 \mathbf{B}_V}{\partial X_m^2} \cdot \mathbf{n} \right)$$

Functional derivatives could be used.

The magnetic field produced by external coils is a functional of coil geometries $\mathbf{x}(X)$

$$\mathbf{B}_V(\bar{\mathbf{x}}) = \frac{\mu_0}{4\pi} \sum_{i=1}^{N_C} I_i \int_{C_i} \frac{d\mathbf{l}_i \times \mathbf{r}}{r^3}$$

Using the functional derivatives, we could retain the **flexibility** of different coil representations.

$$\frac{\partial \mathbf{B}_V}{\partial X_m} = \int_0^{2\pi} \frac{\delta \mathbf{B}_V}{\delta \mathbf{x}} \cdot \frac{\partial \mathbf{x}}{\partial X_m} dt$$

$$\frac{\partial^2 \mathbf{B}_V}{\partial X_m^2} = \int_0^{2\pi} \frac{\delta^2 \mathbf{B}_V}{\delta x^2} \left(\frac{\partial x}{\partial X_m} \right)^2 + \frac{\delta^2 \mathbf{B}_V}{\delta x \delta y} \frac{\partial y}{\partial X_m} \frac{\partial x}{\partial X_m} + \frac{\delta^2 \mathbf{B}_V}{\delta x \delta z} \frac{\partial z}{\partial X_m} \frac{\partial x}{\partial X_m} dt$$

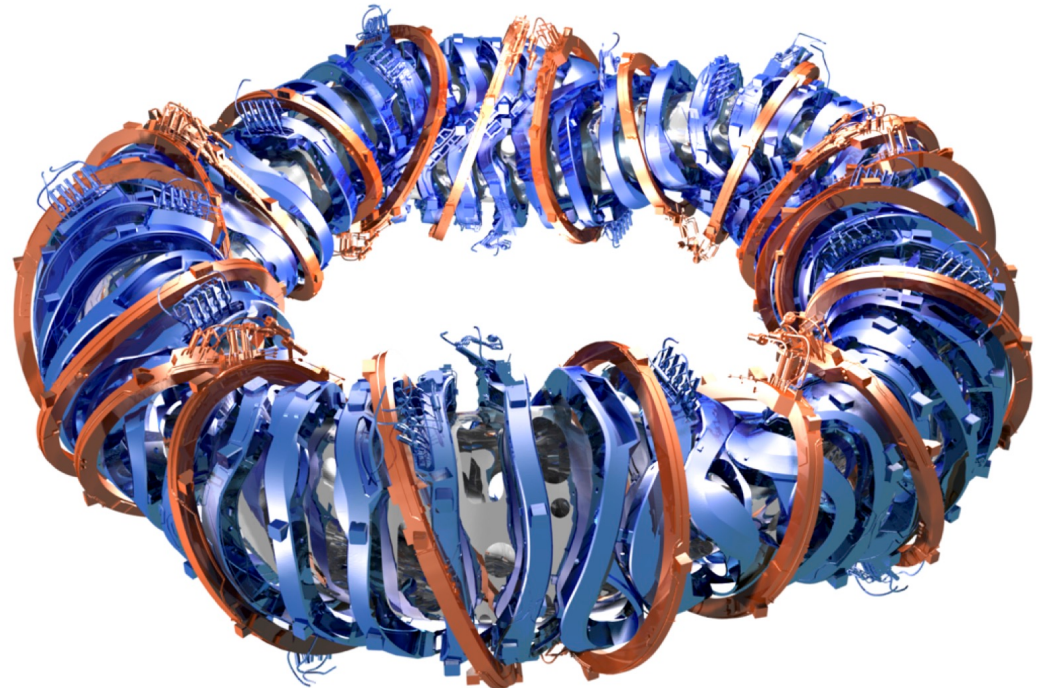
$$\delta^2 \mathbf{B}_V = \frac{\mu_0}{4\pi} I_i \int_0^{2\pi} dt \left[\frac{3[r^2 \mathbf{r} \cdot \delta^2 \mathbf{x}_i + 5(\mathbf{r} \cdot \delta \mathbf{x}_i)^2 - r^2 \delta \mathbf{x}_i \cdot \delta \mathbf{x}_i]}{r^7} (\mathbf{x}_i' \times \mathbf{r}) \right]$$

$$\delta \mathbf{B}_V = \frac{\mu_0}{4\pi} I_i \int_0^{2\pi} dt \left[\frac{3\mathbf{r} \cdot \mathbf{x}_i'}{r^5} \mathbf{r} \times \delta \mathbf{x}_i + \frac{2}{r^3} \delta \mathbf{x}_i \times \mathbf{x}_i' \right. \\ \left. + \frac{3\mathbf{r} \cdot \delta \mathbf{x}_i}{r^5} \mathbf{x}_i' \times \mathbf{r} \right],$$

$$+ \frac{3[r^2 \mathbf{r} \cdot \delta \mathbf{x}_i' + 5(\mathbf{r} \cdot \mathbf{x}_i')(\mathbf{r} \cdot \delta \mathbf{x}_i) - r^2 \delta \mathbf{x}_i \cdot \mathbf{x}_i']}{r^7} (\mathbf{r} \times \delta \mathbf{x}_i) \\ + \frac{9\mathbf{r} \cdot \delta \mathbf{x}_i}{r^5} (\delta \mathbf{x}_i \times \mathbf{x}_i') + \frac{3\mathbf{r} \cdot \delta \mathbf{x}_i}{r^5} (\delta \mathbf{x}_i' \times \mathbf{r}) \\ + \frac{3\mathbf{r} \cdot \mathbf{x}_i'}{r^5} (\mathbf{r} \times \delta^2 \mathbf{x}_i) + \frac{2}{r^3} (\delta^2 \mathbf{x}_i \times \mathbf{x}_i') + \frac{2}{r^3} (\delta \mathbf{x}_i \times \delta \mathbf{x}_i') \left. \right].$$

Speed for calculating the gradient: analytic (5s) VS central difference (574s) (2000 DoF with 32 CPUs)

W7-X modular coils are designed by NESCOIL.



Overview of W7-X coil system including 50 modular coils (blue) and 20 planar coils (red). The planar coils are not used in the standard configuration.

From <http://fusion.rma.ac.be/research.php?subj=W7X>

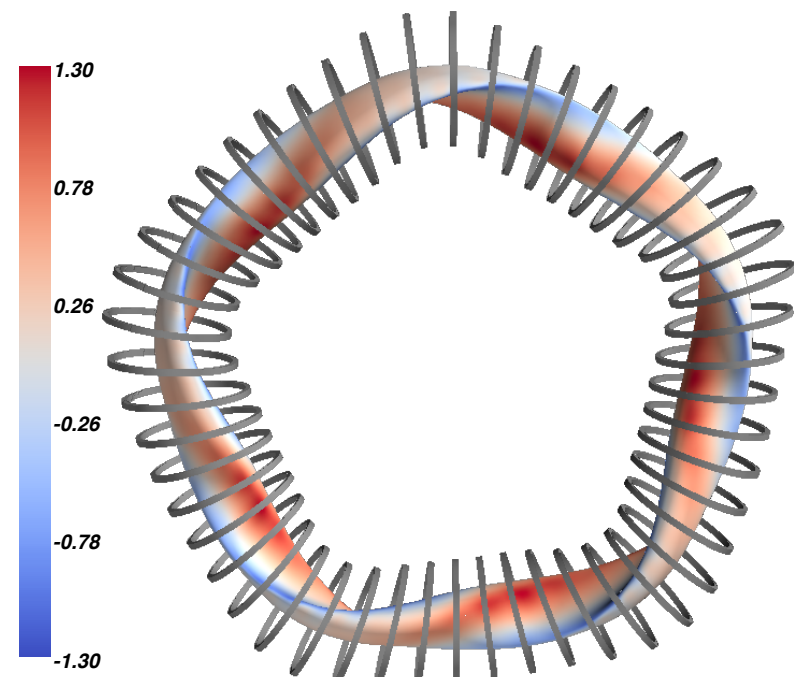
How do the modular coils come from?

NESCOIL on an optimized winding surface satisfying: (*Beidler et al., FST, 1989*)

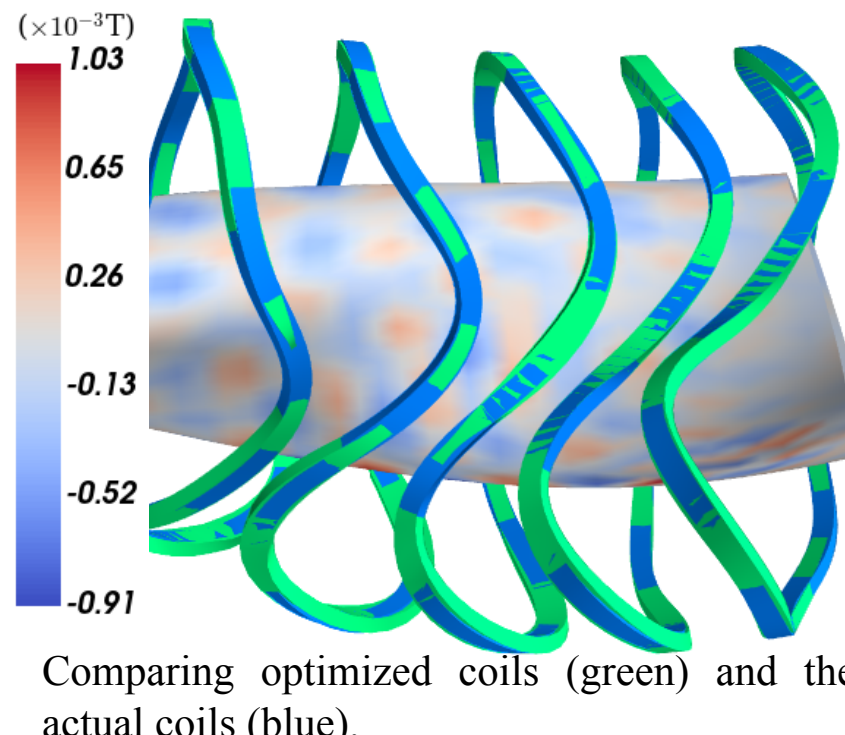
- ✓ maximum distance between the plasma and the coils
- ✓ maximum distance between two adjacent coils
- ✓ maximum radius of curvature of the coils
- ✓ quality of the resulting magnetic field with respect to the given field.

Designing W7-X stellarator coils from circular initialization.

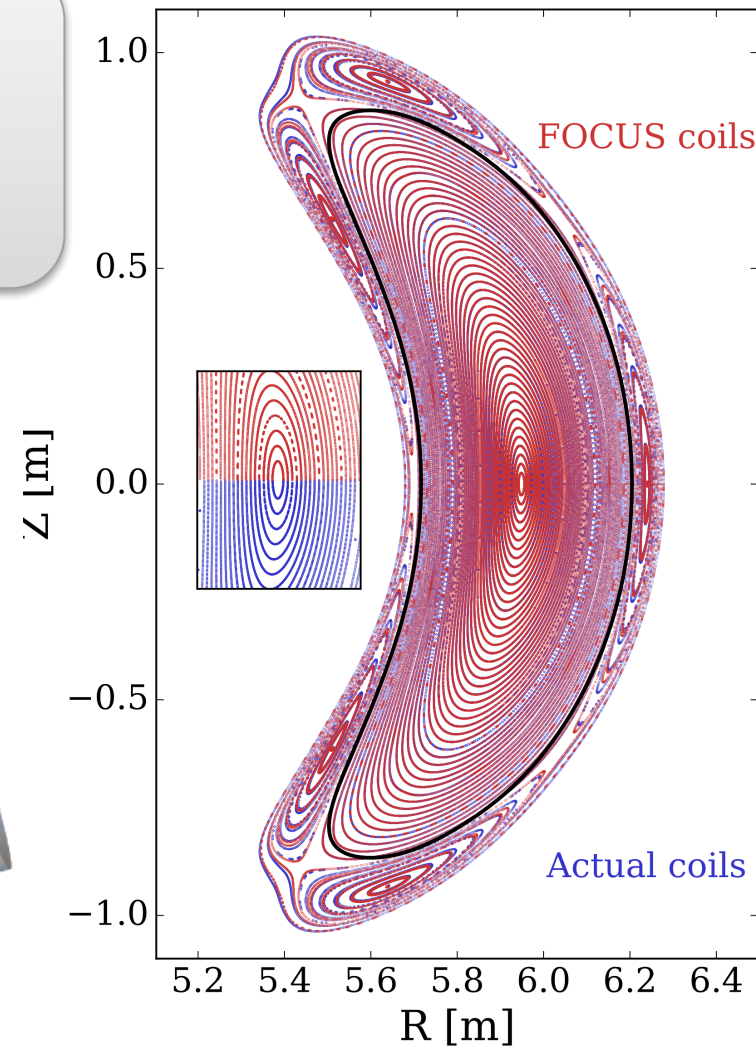
- ❖ **Target boundary:** LCFS from the standard configuration with known B_n calculated from the actual coils
- ❖ **Initial guesses:** 50 circular coils ($r = 1.25\text{m}$) equally placed surrounding the plasma;
- ❖ **Optimizer:** 50 iterations Nonlinear Conjugate Gradient (CG) + 50 iterations Modified Newton method (MN);
- ❖ **Computation time:** $\sim 3.6\text{h}$ with 128 CPUs (without enforcing periodicity and stellarator symmetry)



Input plasma boundary, $\mathbf{B} \cdot \mathbf{n} - T_{Bn}$ distribution (colors) and the initial circular coil (grey).

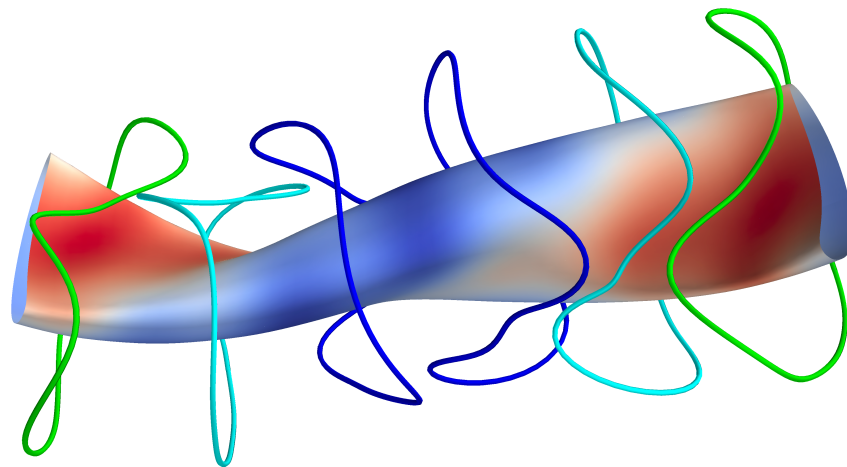


Comparing optimized coils (green) and the actual coils (blue).

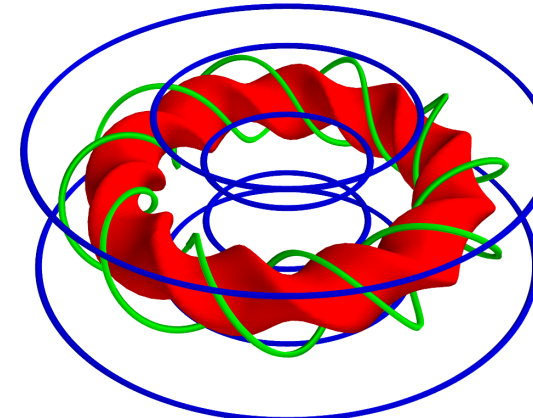


The average relative iota deviation is **0.028%**.

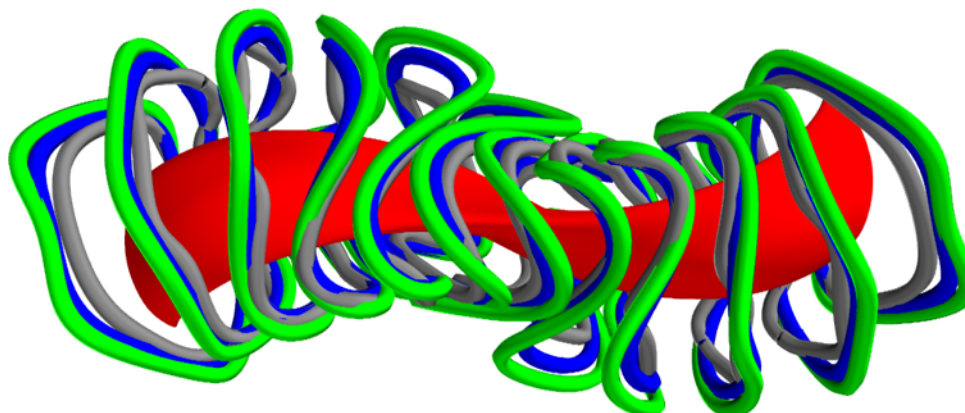
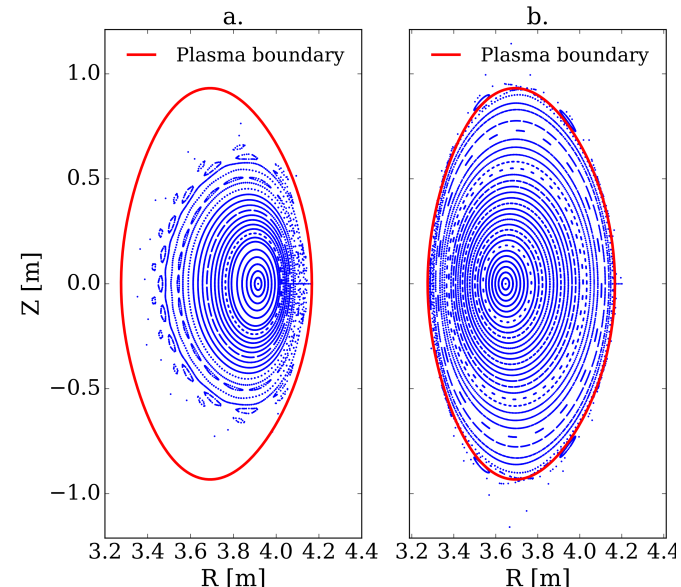
FOCUS is compatible to various configurations and coils.



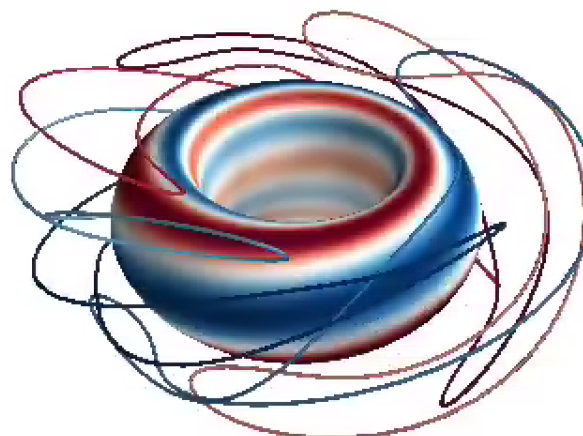
30 coils (6/period) solution for W7-X without significant sacrifices in magnetic field.



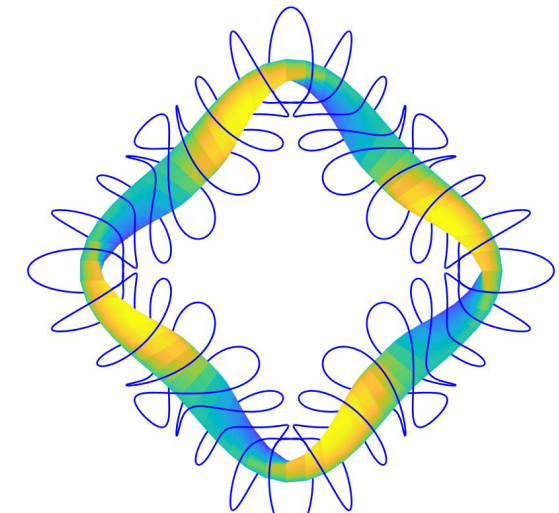
Mitigate error fields in LHD caused by numerical parameterization.



Improved coil set for HSX with larger coil-plasma separation and less magnetic ripple.



Onset RMP coils for DIII-D.
(Logan & Zhu, APS 2017)



Helical coils for HSX
(Kruger et al., APS 2017)

Hessian method for EF sensitivity

Zhu, et al. Plasma Physics and Controlled Fusion 60 (2018) 054016

Quadratic approximation of the error field caused by coil deviations.

❖ Normalized residual B_n errors on target flux surface measure error fields.

- Ideally, $F=0$, global minimum, coils perfectly produce the magnetic field.
- Generally, the lower F , the better approximation to the desired \mathbf{B} .

$$F(\mathbf{X}) \equiv \int_S \frac{1}{2} \left(\frac{\mathbf{B} \cdot \mathbf{n}}{|\mathbf{B}|} \right)^2 ds \quad \mathbf{X}: \text{coil parameters}$$

❖ Taylor expansion

$$F(\mathbf{X}) = F(\mathbf{X}_0) + (\mathbf{X} - \mathbf{X}_0)^T \cdot \mathbf{g}_0 + \frac{1}{2} (\mathbf{X} - \mathbf{X}_0)^T \cdot \mathbf{H}_0 \cdot (\mathbf{X} - \mathbf{X}_0) + \dots$$

When \mathbf{X} is **near a local minimum** \mathbf{X}_0 , only the quadratic term is left.

Any arbitrary deviations can be composed in eigen-space.

$$\Delta \mathbf{X} = \sum_i a_i \mathbf{v}_i \quad \mathbf{v}_i^T \mathbf{H}_0 \mathbf{v}_i = \lambda_i, \quad (i = 1, \dots, N \text{ and } \lambda_i \geq 0)$$

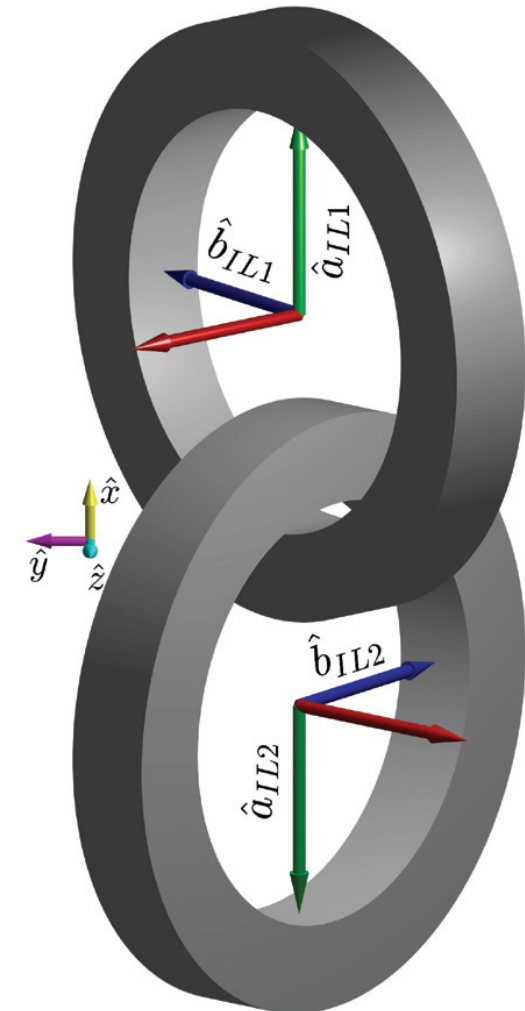
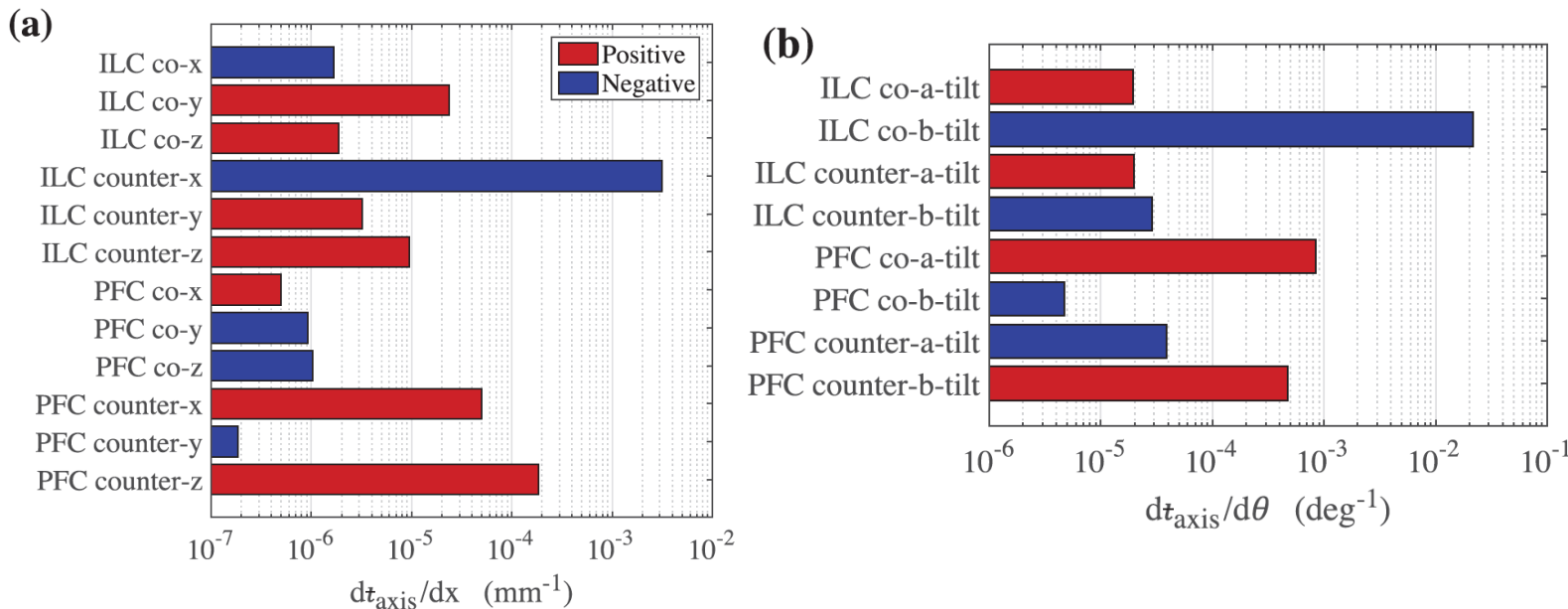


Error field:

$$\boxed{\Delta F(\mathbf{X}) \approx \frac{1}{2} \sum_i^N a_i^2 \lambda_i}$$

Previous studies show CNT is more sensitive to IL coil displacements.

- ❖ Hammond *et al.* (*PPCF*, 2016) carried out an excellent study on analyzing the error fields of CNT. They calculated the derivatives of ι_{axis} with respect to manually-defined rigid displacements with finite difference.



- ❖ Conclusion: **The separation of the IL coils** (along the negative \hat{x} axis) and **the tilt angle between the IL coils** (clock-wise around \hat{b}) have the greatest influences.
- ❖ Similar results were obtained by earlier investigations by evaluating the quality of magnetic surface and plasma volume (*Pedersen et al. 2006*).

Ten defined rigid displacements for IL coils.

Hessian matrix method used on the CNT-like configuration.

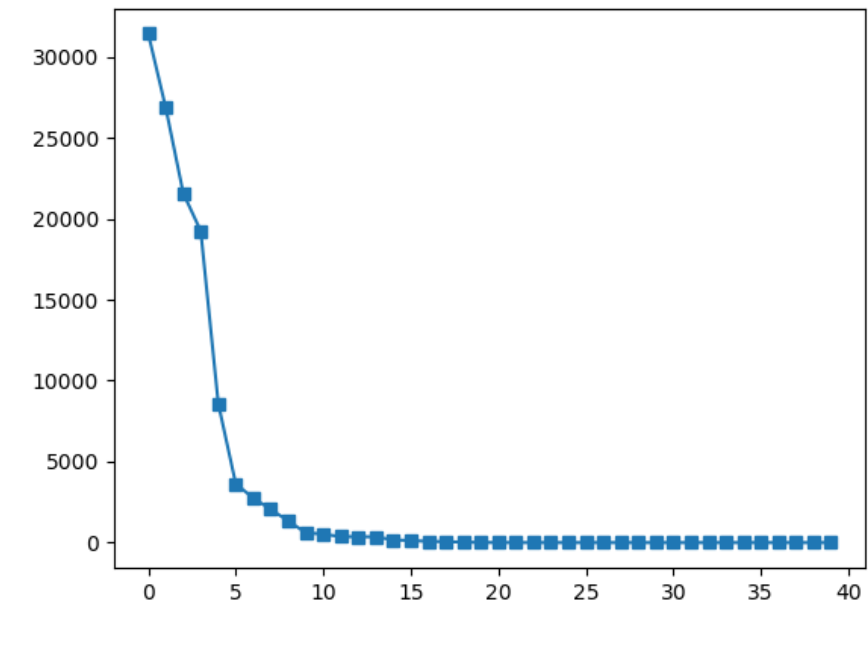
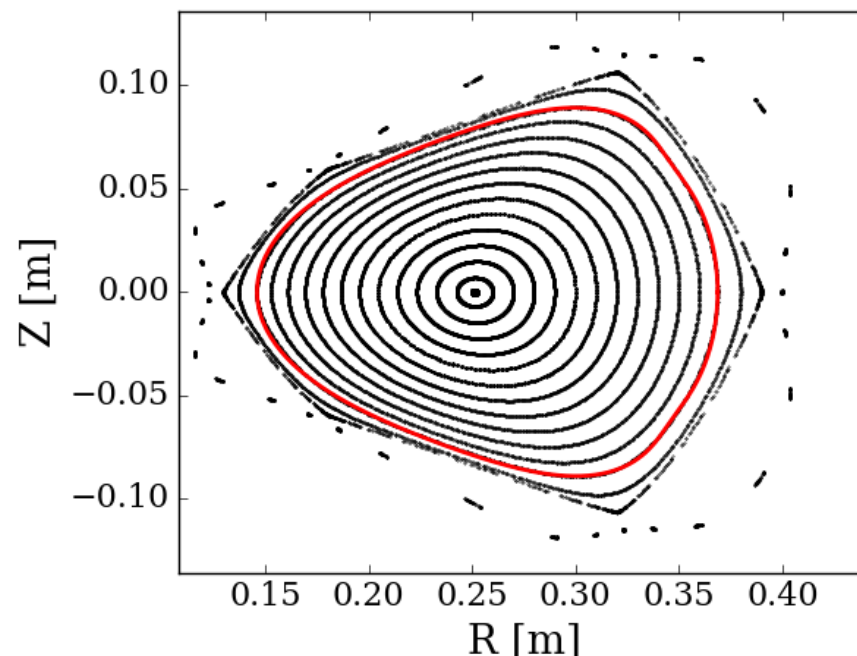
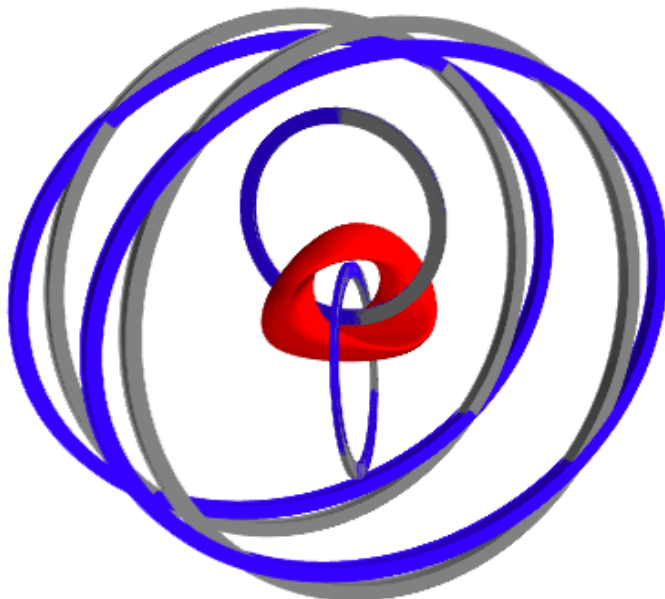
CNT-like: A fitted vacuum flux surface produced by actual coils.

1. Find the minimum (coil optimization)

- $N_F=1$ to enforce planar coils;
- use the Truncated Newton method to design coils ($F = 10^{-5}$; $|g| = 10^{-11}$)

2. Eigenvalue decomposing of the Hessian

3. Apply eigenvectors to analyze coil deviations

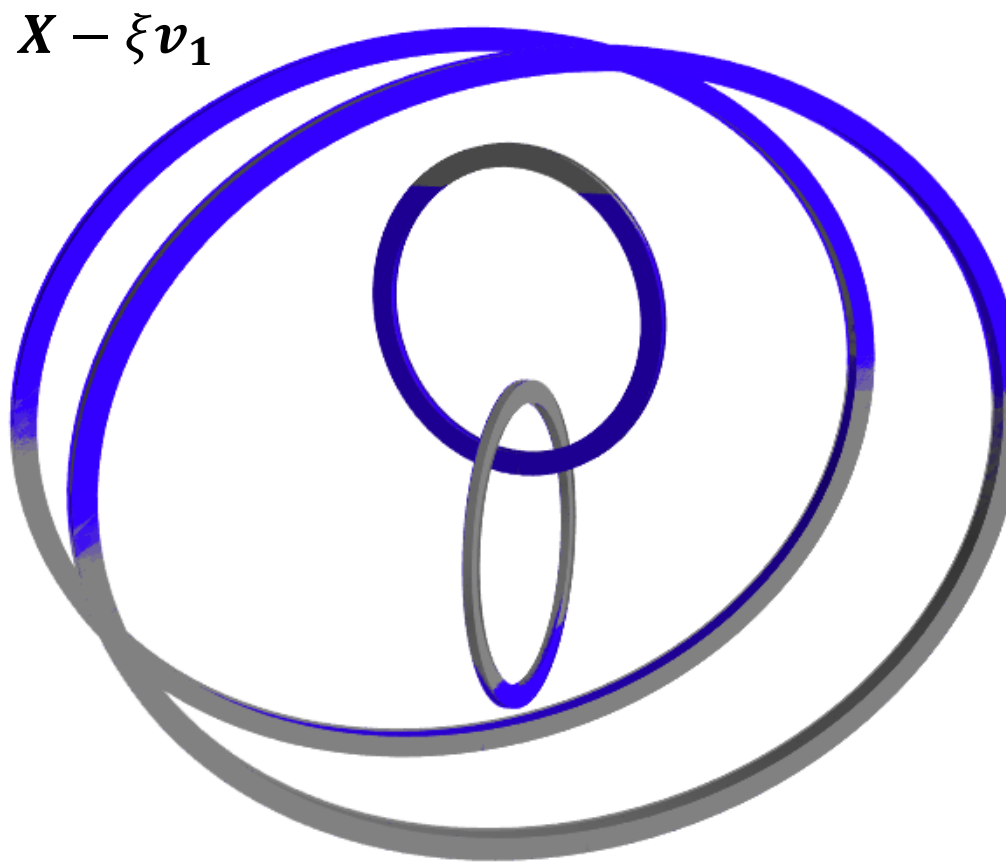


The first principal eigenvector has large impact on EF.

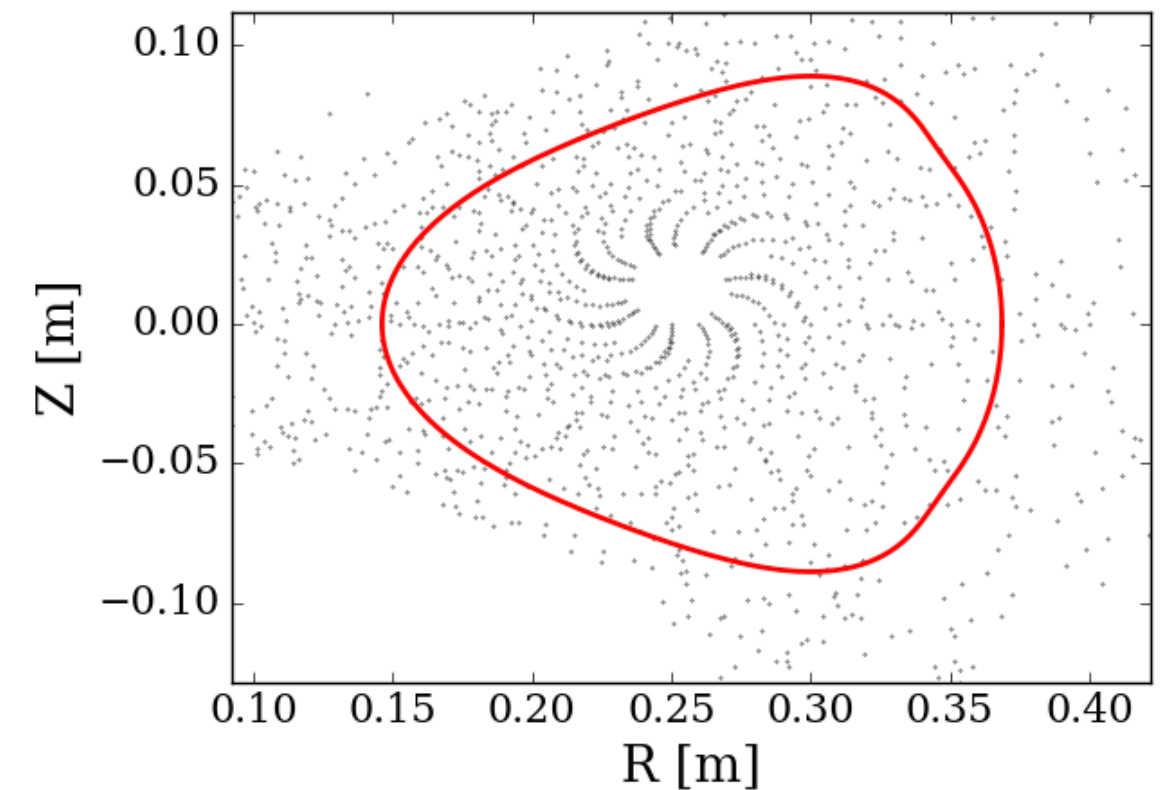
Apply a small perturbation:

$$|\Delta \mathbf{X}| = \sum a_i^2 = \xi = 0.01$$

Coils visually indistinguishable



Significant changes in magnetic surfaces



Grey: equilibrium coils; Blue: perturbed coils

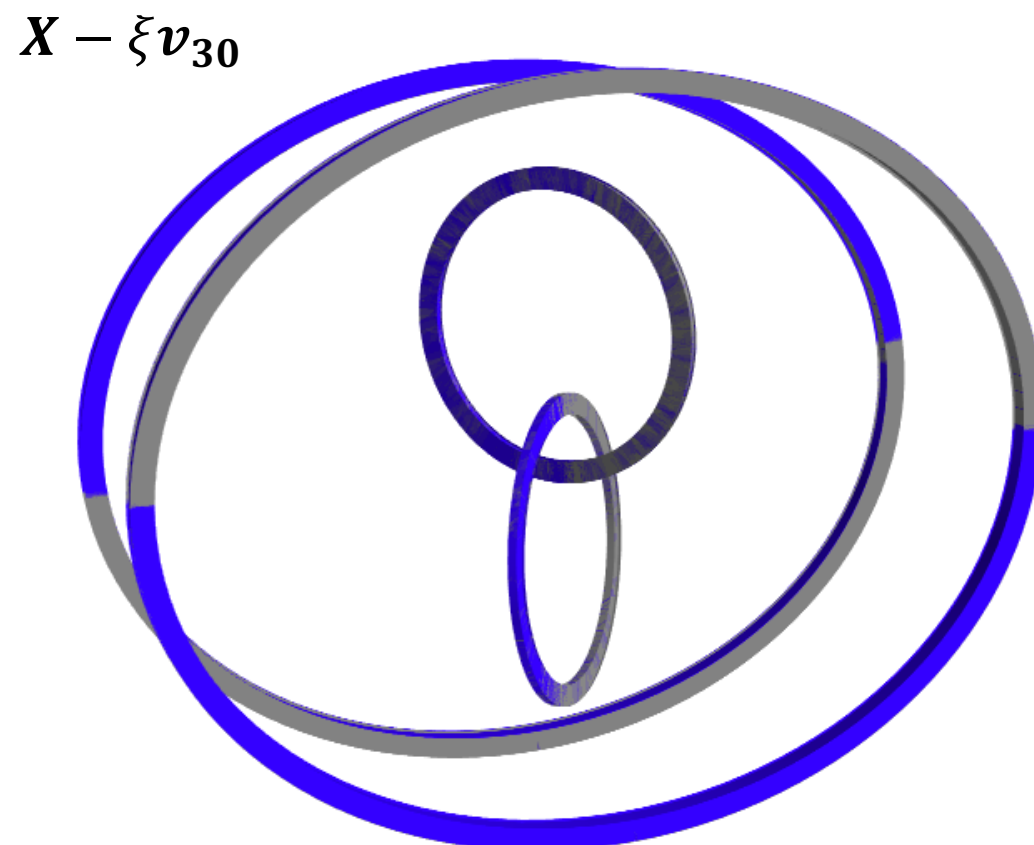
Poincare plots in vacuum field produced
by perturbed coils.

The 30-th principal eigenvector has much less impact.

Apply a small perturbation:

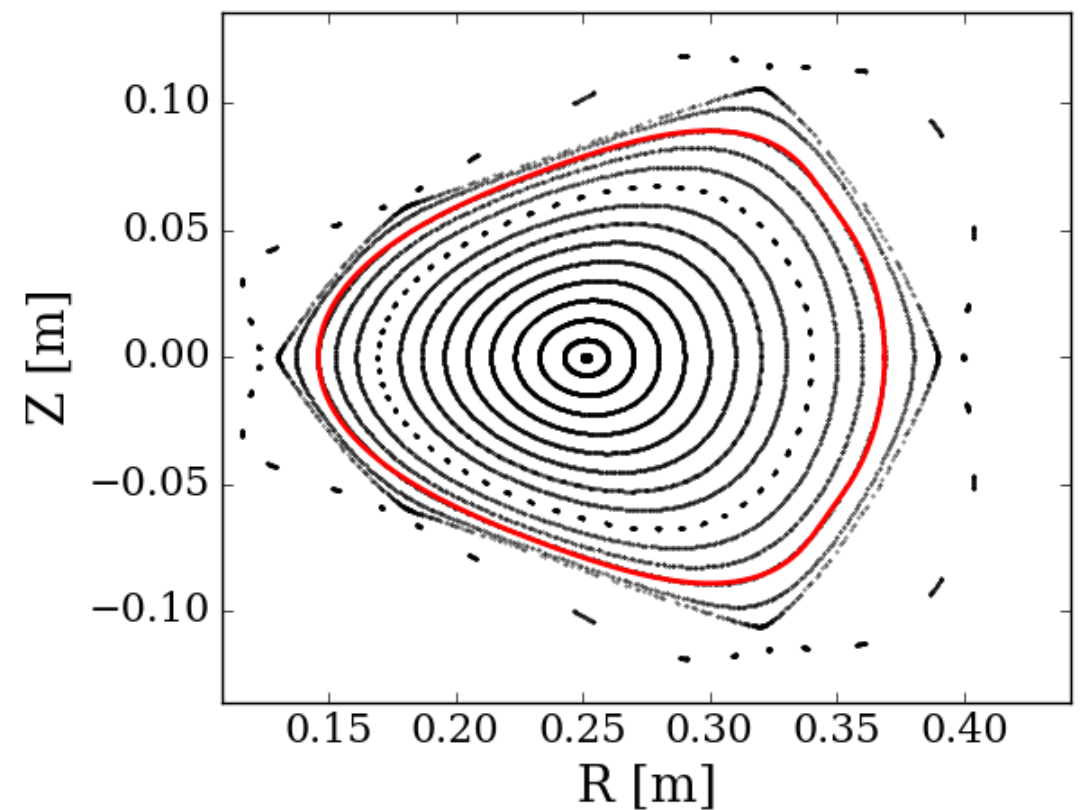
$$|\Delta \mathbf{X}| = \sum a_i^2 = \xi = 0.01$$

Coils visually indistinguishable



Grey: equilibrium coils; Blue: perturbed coils

Negligible changes in magnetic surfaces



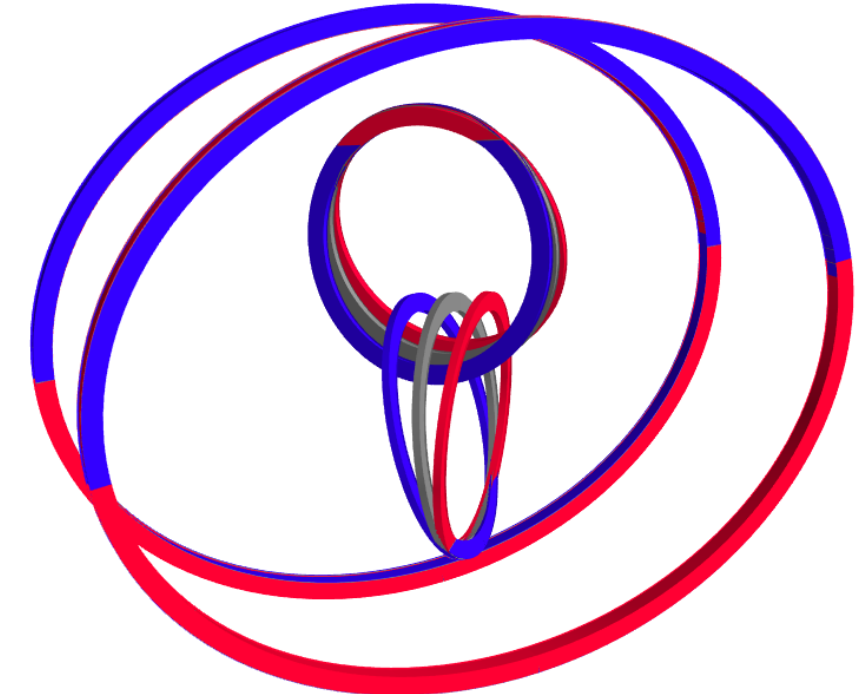
Poincare plots in vacuum field produced by perturbed coils.

Interlinked parts are the most dangerous region.

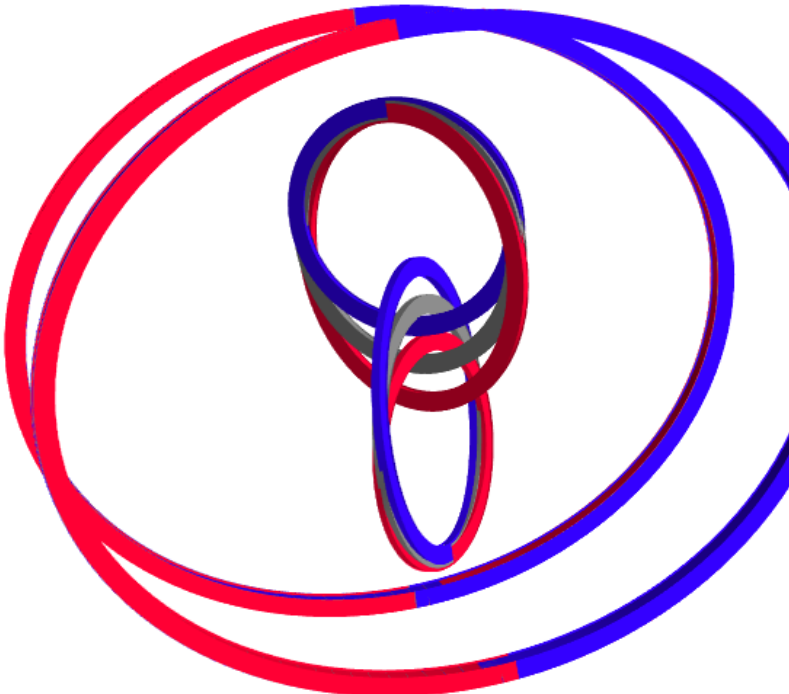
Apply a larger perturbation:

$$|\Delta \mathbf{X}| = \sum a_i^2 = \xi = 0.5$$

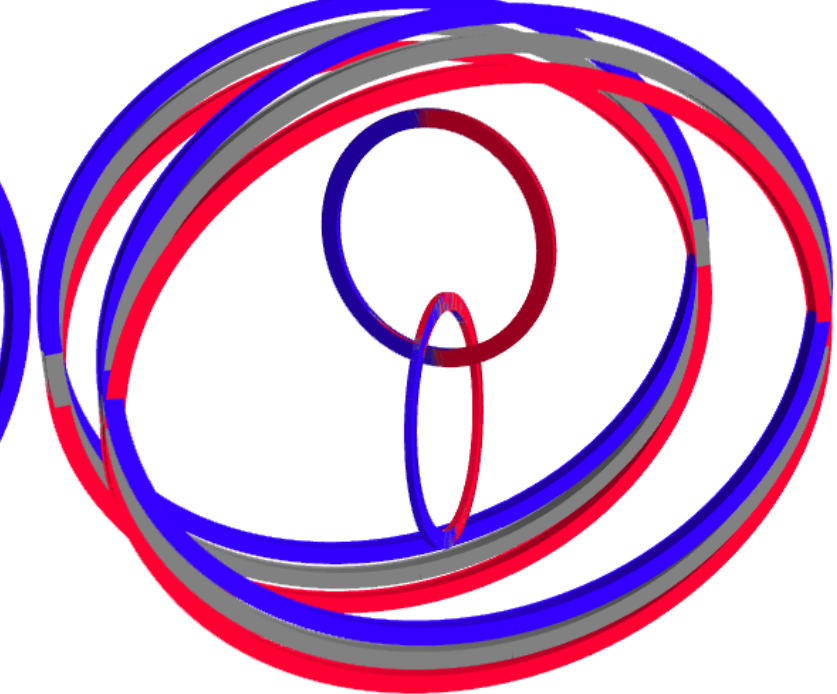
$X \pm \xi v_1$



$X \pm \xi v_2$



$X \pm \xi v_{30}$



The perturbed coils under the different principal eigenvectors. The equilibrium coils, negatively perturbed coils and positively perturbed coils are in grey, blue and red respectively.

Error field sensitivity of the CNT-like configuration.

- ❖ **EF is sensitive to the interlinked parts.**

tilt or stretch / compress the interlinked part will cause significant EF.

- ❖ **Helmholtz coils have much larger tolerance.**

EF is insensitive to Helmholtz coils.

- ❖ **Coil current deviations can also cause EF.**

ν_2 has an effect to change the currents in IL coils by 10.37% ($\xi = 1.0$).

- ❖ **Other points:**

- Computation time: 0.42s for calculating the Hessian with 32 CPUs.
- Not only rigid displacement is considered, but also elliptical deformations.
- By increasing N_F , theoretically allow all the possible deformations, even local ones.
- Only valid when near the minimum, otherwise the linear term is not negligible.

Summary

- ❖ **Introduced a new method for designing stellarator coils, with two new features:**

- more flexible by getting rid of the “winding surface”
- more robust and faster by employing analytically calculated derivatives

- ❖ **Demonstrated an fast/simple method to analyze coil sensitivities using the Hessian method.**

CNT-like results are consistent with previous work by using numerical calculations.

Sensitivity analysis used for better controlling error fields, reducing cost and saving time.

- ❖ **Ongoing work:**

Applied in the design of CFQS (China’s first QA stellarator) and other devices.

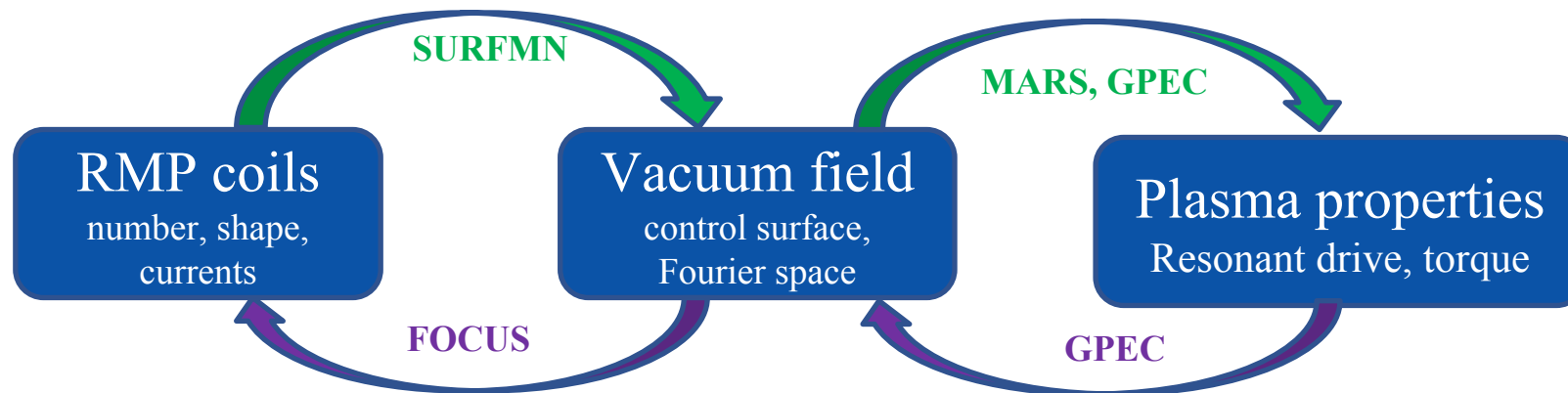
Incorporated with plasma sensitivity.

Analyzing local sensitivity by local representations and/or shape gradient/Hessian.

Backup slides

Exploring new RMP coil designs in Tokamaks using FOCUS.

- ❖ Find a path from the target plasma properties to appropriate coils.

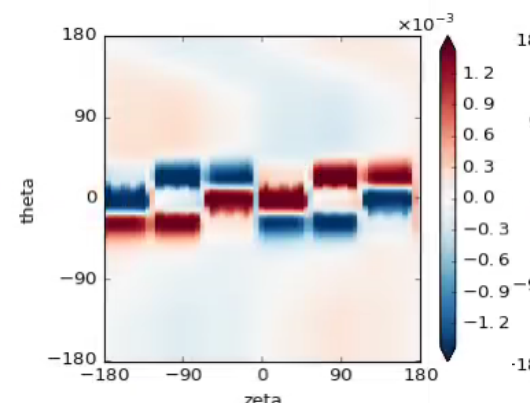
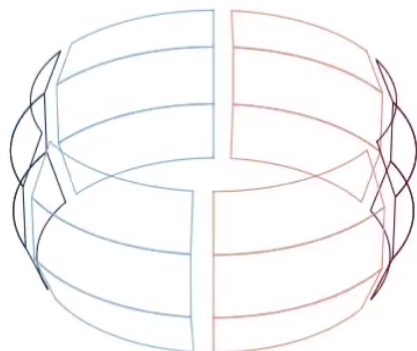


FOCUS can optimize the coils to meet the target magnetic spectrum from GPEC

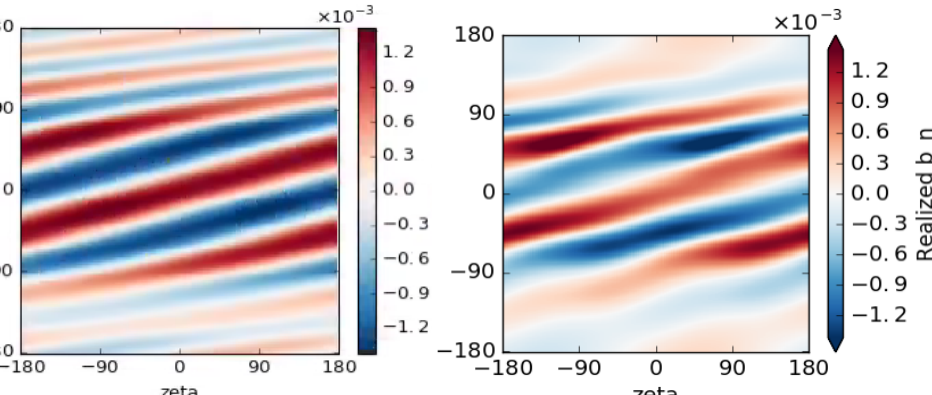
$$f_H = \frac{1}{2} \sum_{m,n} w_{mn}^H |\Delta_{mn} - \Delta_{mn}^o|^2$$
$$\Delta_{mn} = \int_S (\mathbf{B} \cdot \mathbf{n}) e^{-i(m\theta - n\zeta)} ds$$

- ❖ Applying FOCUS to design RMP coils satisfying the 1st dominant mode of the resonant coupling matrix, calculated from GPEC.

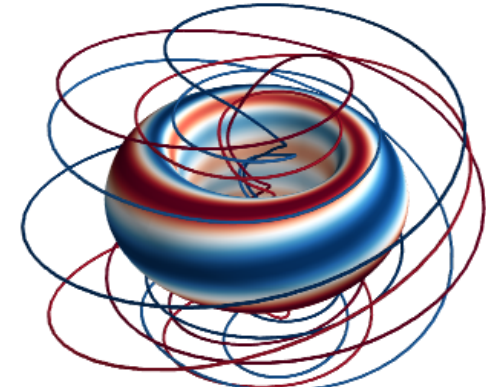
Optimize current distribution in regular window-pane coils (62% overlap)



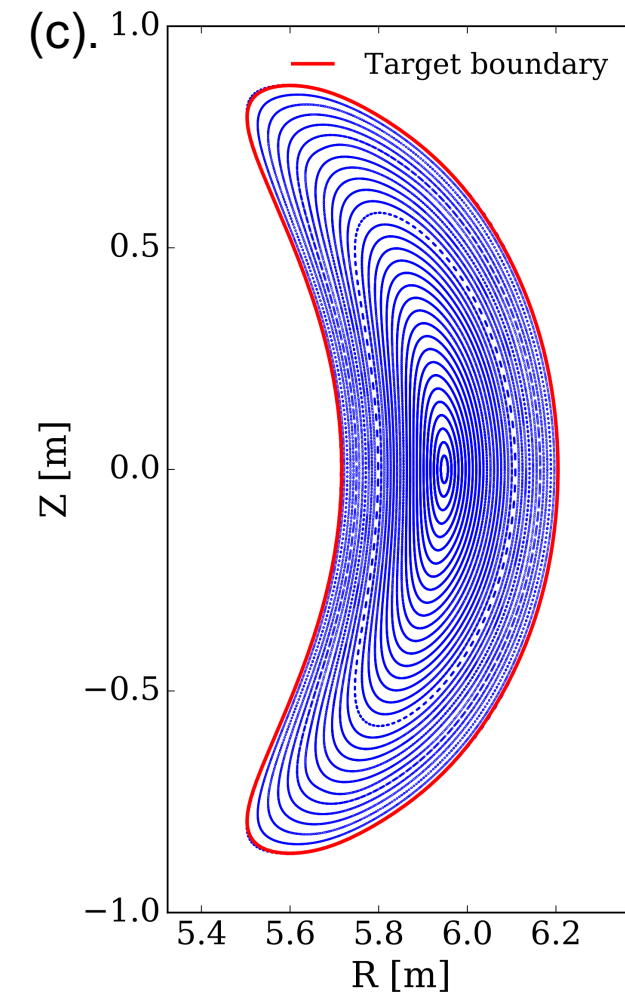
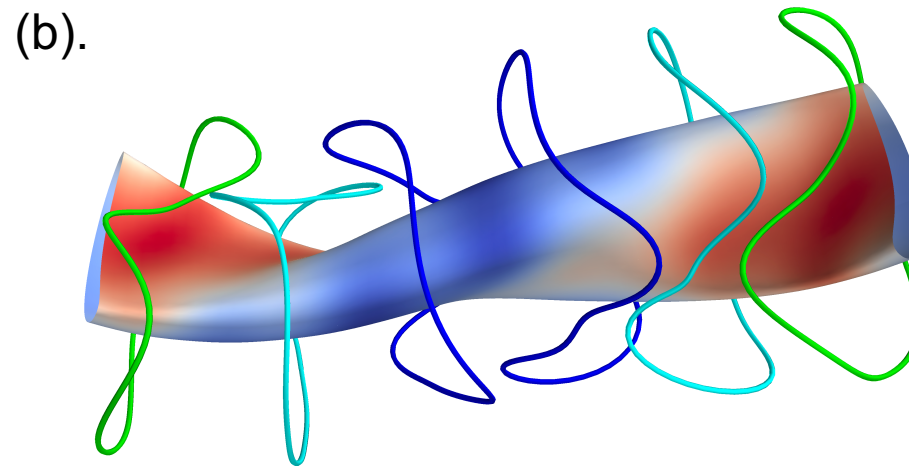
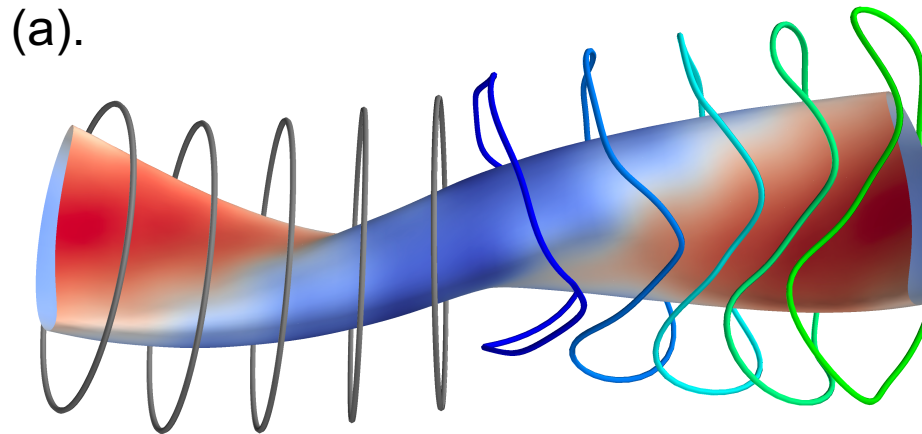
Target ideal dominant mode spectrum



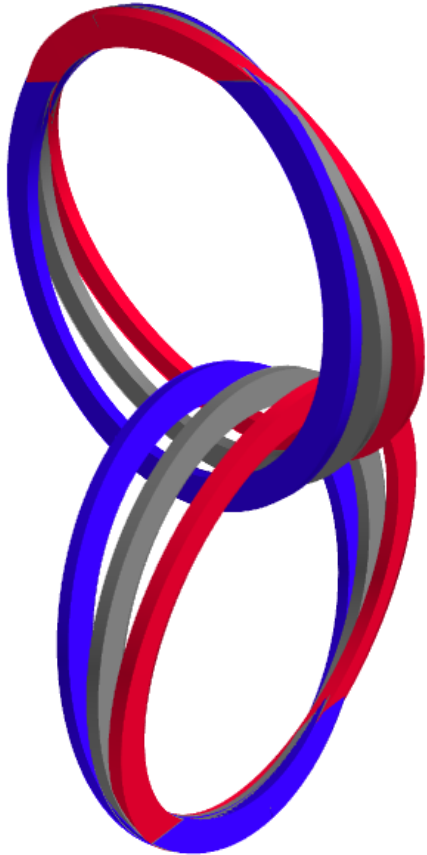
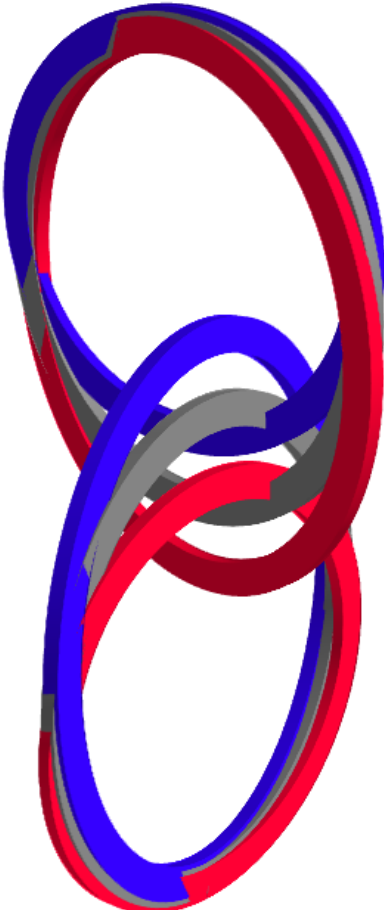
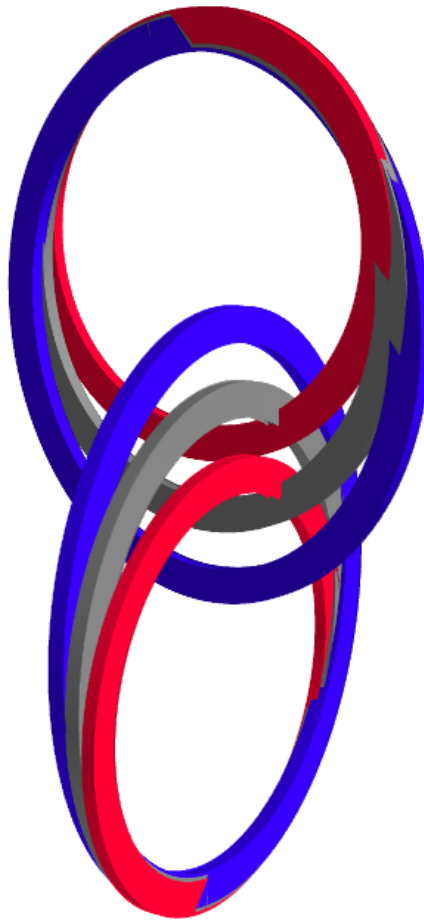
Try some “art-like” helical coils (92% overlap)



Interesting study of reconstructing W7-X with as few as 30 coils.



(a). FOCUS optimized 50 coils (half period initial coils and half final coils are plotted); (b). 30 coils solution; (c) Poincare plots of the vacuum field produced by 30 coils compared with the target plasma boundary. The color on the surfaces indicated the B magnitude produced by external coils. Further explorations on the magnetic ripple, transport, etc. should be carried out.

$X_0 + \xi v_1$  $X_0 + \xi v_2$  $X_0 + \xi v_3$  $X_0 + \xi v_4$ 